ELEMENTAL QUANTIFICATION OF A STEM SAMPLE WITH VARYING THICKNESS

Julien Aubourg[1*], Meiken Falke[1]

[1]Bruker Nano GmbH, Electron Microscope Analyzers, Am Studio 2D, 12489, Berlin, Germany

[*]julien.aubourg@bruker.com

Quantitative elemental analysis by scanning transmission electron microscopy combined with energy dispersive X-ray spectroscopy (STEM EDS) is essential for nanoscale materials characterization, yet its accuracy is often limited by specimen thickness and Xray absorption, especially in materials containing both light and heavy elements such as ZnO. Here, we evaluate the influence of specimen thickness on quantitative EDS. A wedge-shaped electron transparent lamella containing a ZnO layer with an expected 50:50 Zn:O composition was prepared by focused ion beam milling. STEM EDS measurements were performed at 200 kV, and an elemental line profile across the ZnO layer was quantified using standardless Cliff-Lorimer, standard-based Cliff-Lorimer, and Zeta-factor methods (available in the ESPRIT software). Cliff-Lorimer approaches exhibit thickness-dependent deviations, with oxygen increasingly underestimated in thicker regions. In contrast, only the Zeta-factor method yields a constant Zn:O ratio matching the expected stoichiometry. Based on these results we discuss under which conditions the Zeta-factor method can enable reliable, thickness-independent quantitative EDS.

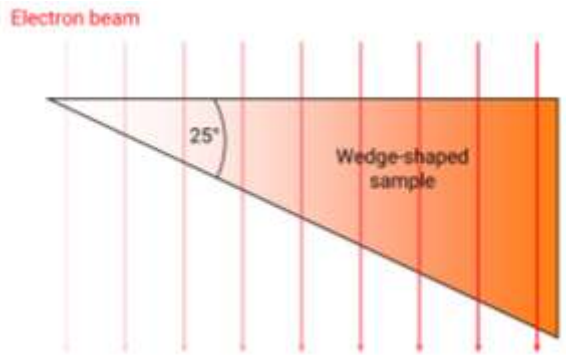

Fig. 1: Side-view diagram of the wedge-shaped sample. During the EDS analysis, the electron beam probes regions of increasing thickness.

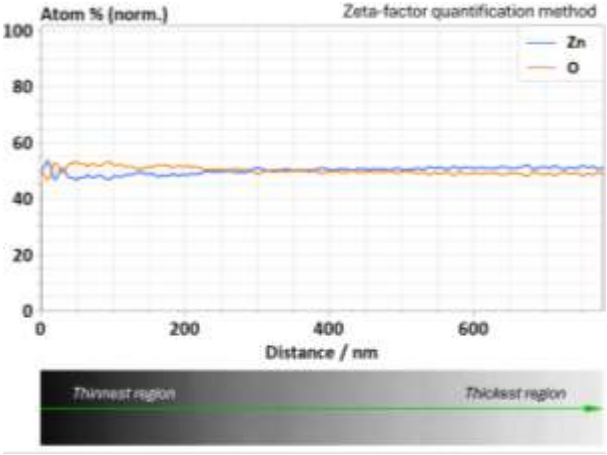

Fig. 2: Atomic concentration along a line profile acquired over a $Zn_{0.5}O_{0.5}$ electron-transparent sample of increasing thickness using the Zeta-factor quantification methods.
Sample and data courtesy: X. Jin, *KIT*

References:
[1] X. Jin et al., “Improvement of Quantitative STEM/EDXS Analyses for Chemical Analysis of Cu(In,Ga)Se2 Solar Cells with Zn(O,S) Buffer Layers,” Microscopy and Microanalysis, vol. 29, no. 1, pp. 69–77, Feb. 2023, doi: 10.1093/micmic/ozac031.
[2] X. Jin et al., “Improved quantitative chemical analyses of Cu(In,Ga)Se_2 solar cells performed by STEM/EDXS,” Microsc Microanal, vol. 27, no. S1, pp. 2060–2063, Aug. 2021, doi: 10.1017/S1431927621007467.

Leveraging Machine Learning for Advanced Nanoscale X-ray Analysis: Unmixing Multicomponent Signals and Enhancing Chemical Quantification

Hui Chen[1*], Duncan T.L. Alexander[2], Cécile Hébert[2]

[1]Catalan Institute of Nanoscience and Nanotechnology (ICN2), CSIC and BIST, Campus UAB, Bellaterra, 08193 Barcelona, Catalonia, Spain
[2]Electron Spectrometry and Microscopy Laboratory (LSME), IPHYS, EPFL, Lausanne, Switzerland

[*]hui.chen@icn2.cat

Energy dispersive X-ray (EDX) spectroscopy in the transmission electron microscope is a key tool for nanomaterials analysis, providing a direct link between spatial and chemical information. However, using it for precisely determining chemical compositions presents challenges of noisy data from low X-ray yields and mixed signals from phases that overlap along the electron beam trajectory. To address these limitations, we develop PSNMF (non-negative matrix factorization based pan-sharpening) [1], an innovative machine learning approach that enhances STEM-EDX analysis by simultaneously separating overlapping phases and reconstructing a high-quality dataset. By leveraging the Poisson nature of EDX spectral noise and binning operations, PSNMF retrieves high-quality phase spectral and spatial signatures via consecutive non-negative matrix factorizations (NMF), enabling precise and robust dataset reconstruction.

We validate PSNMF using synthetic datasets with varying noise levels, as well as experimental STEM-EDX data from nano-mineralogical samples and Au-Cu2O catalytic nanoparticles. These datasets represent two major categories of samples commonly analyzed in STEM-EDX: 1) lamellae of uniform thickness that are prepared from bulk materials using ion beam milling and/or mechanical thinning; 2) nanostructures of irregular thickness that are supported on amorphous carbon films. Our results demonstrate that PSNMF not only obtains accurate phase signatures, outperforming the benchmark method, NMF, in identifying minor phases within complex materials, but also reconstructs datasets with significantly lower noise and higher fidelity than the benchmark denoising method, principal component analysis (PCA), particularly for trace element quantification. The superior phase decomposition accuracy and enhanced clarity of the denoised elemental maps highlight PSNMF's strong potential for improving STEM-EDX analytics across a variety of nanoscience domains.

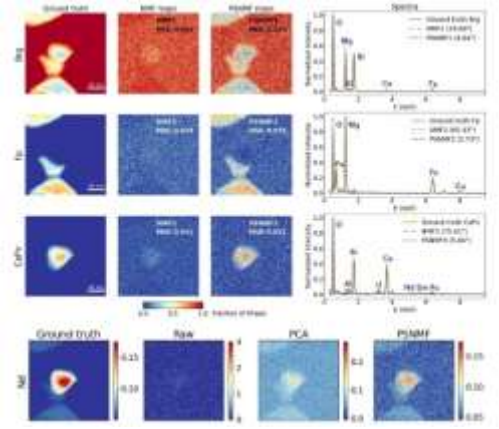

Fig. 1: PSNMF applied to a simulated data set having a very low SNR (average of 18 X-ray counts per pixel), compared to standard NMF for phase identification and to PCA for data set denoising.

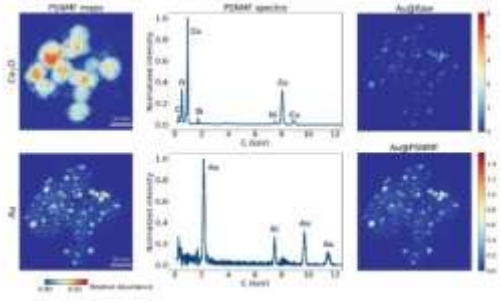

Fig. 2: PSNMF applied to an experimental 512 × 512 pixel data set that was acquired from Au−Cu2O nanoparticles supported on a carbon film.

References:

[1] H. Chen, D. T. L. Alexander, C. Hébert, Nano Lett. **24**, 10177–10185 (2024).

ELUCIDATING IMPACT OF NOVEL DISEASES AND OCEAN ACIDIFICATION ON CORAL SKELETONS

Paul Smeets[1*], Yu Wen[1], Vivian Merk[2], Yongfa Cheng[1], Xiaobing Hu[1], Vinayak Dravid[1]

[1]Northwestern University, Materials Science & Engineering, Evanston, IL, USA
[2]Florida Atlantic University, Department of Chemistry and Biochemistry, Boca Raton, FL, USA

[*]paul.smeets@northwestern.edu

Scleractinian corals build highly ordered aragonite ($CaCO_3$) skeletons vital for marine ecosystems, but face multiple challenges through global climate change, unsustainable human activity, and coral-specific diseases. Stony Coral Tissue Loss Disease (SCTLD) has recently emerged as one of the most destructive coral diseases [1], however, its potential impact on skeleton mineralization has not yet been explored. We use a multiscale electron microscopy approach to characterize healthy and SCTLD-afflicted skeletons (Fig 1). On the micro-scale, we find calcite next to spherulitic aragonite fibers radiating from centers of calcification (CoC) in healthy coral, while no calcite persists in diseased coral. At the nanoscale, a healthy CoC contains aragonite grains together with pockets of amorphous calcium carbonate (ACC). In contrast, 4D STEM data reveals diseased coral also contains calcite and calcium carbonate hemi-hydrate (CCHH) nanoparticles. HRTEM and STEM imaging show planar defects along aragonite [100]. In healthy coral, a planar feature parallel to the (001) plane (bright in ABF) exhibits no corresponding contrast in HAADF, indicating continuity of the Ca sublattice with localized modification of carbonates. In diseased coral, HAADF images suggest Ca depletion. Alltogether, we find SCTLD alters skeletogenisis.
Moreover, coral growth is expected to decrease as oceans become more acidic due to the uptake of anthropogenic CO_2. We have developed an in-situ platform to potentially address how corals can be affected through this process. Through initial introduction of water vapor, and introduction of CO_2 gas as a second to lower the local pH, we were able to dissolve aragonite particles as a proof of principle (Fig. 2a-f). By preparation of sections of corals sandwiched between SiN_x-based chips (Fig 2g-h), we intend to explore coral dissolution mechanisms as a proxy for ocean acidification at the nanoscale.

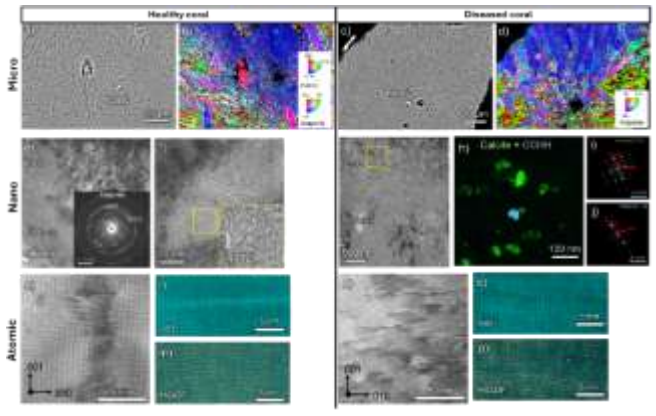

Fig. 1: a,b) SEM image & EBSD map of healthy, and c,d) diseased coral. e,f) TEM images of healthy, and g) TEM image and h-j) 4D STEM data of diseased coral. k-m) HRTEM, ABF & HAADF image of healthy coral, and n-p) diseased coral

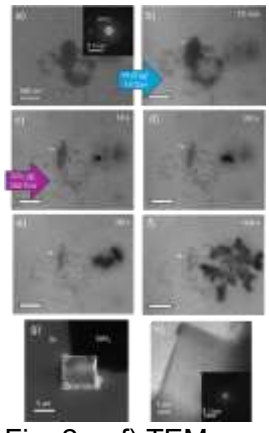

Fig. 2: a-f) TEM snapshots showing dissolving aragonite particles (white arrow); growing crystals (red arrow). g) SEM and h) TEM image of coral lamella on SiN_x chip

References:
[1] E.M. Muller et al., Front. Mar. Sci. **7**, (2020).

UNDERSTANDING THE MECHANISM OF COLORATION AND MATERIALS OPTIMIZATION IN RODENT TEETH

Vesna Srot[1*], Gregor Kapun[2], Felicitas Predel[1], Birgit Bussmann[1], Boštjan Pokorny[3], Elena Buzan[4], Bernhard Fenk[1] and Peter A. van Aken[1]

[1]Max Planck Institute for Solid State Research, 70569, Stuttgart, Germany
[2]National Institute of Chemistry, 1000, Ljubljana, Slovenia
[3]Faculty of Environmental Protection, 3320, Velenje, Slovenia
[4]University of Primorska, 6000, Koper, Slovenia

[*]V.Srot@fkf.mpg.de

Teeth represent a unique natural composite material, incorporating optimally arranged, closely intertwined simple inorganic and organic compounds. The continuously growing elongated rodent incisors display adaptations and optimizations that surpass those of human teeth. They can be identified by their orange-brown color and their particular construction, in which hard enamel covers only the labial side of the incisor, rendering the tooth self-sharpening [1]. Fully formed enamel consists of approximately 96 wt% elongated hydroxyapatite (HA) crystals, with the remaining being organic material and water [2].

In this study [3], we followed the structural and chemical development of rodent incisors from seven species (beaver, coypus, marmots, squirrels, voles, rats and mice) from macro-scale to nano-scale.

We primarily recognized ferritin nanoparticles filling ameloblasts during their pigmentation stage. The crystalline ferrihydrite nanocore, with Fe in a 3+ oxidation stage, indicates an iron storage mechanism that protects cells from potential toxicity.

Furthermore, iron-rich material from ameloblasts infiltrates the outer layer of the radial enamel that occupies the empty spaces between elongated HA crystals (Fig. 1a). The infiltrated iron-rich material forms a connected 3D network that represents a secondary phase with a ferrihydrite-like composition (Fig. 1b). This results in the creation of iron-rich enamel (Fe-EN).

Finally, we discovered an inorganic-organic surface layer (SL) formed parallel to the surface of the incisors for all examined species (Fig. 2a). Fine structural details of Fe-$L_{2,3}$ ELNES reveal that iron is in a predominantly 3+ oxidation state (Fig. 2b). We examined the evolution of the SL from the non-erupted part to its fully developed state in the erupted part of the incisor. Moreover, we noticed a direct correlation between the color of the rodent incisor and the thickness of the SL. Consequently, we propose replacing the term ``pigmented enamel`` with ``iron-rich enamel (Fe-EN)``.

Our findings have significant implications for the development of dental materials and the potential for innovations in restorative dentistry.

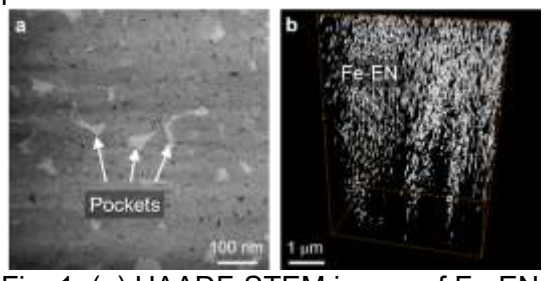

Fig. 1: (a) HAADF-STEM image of Fe-EN; (b) 3D reconstruction of pockets in Fe-EN.

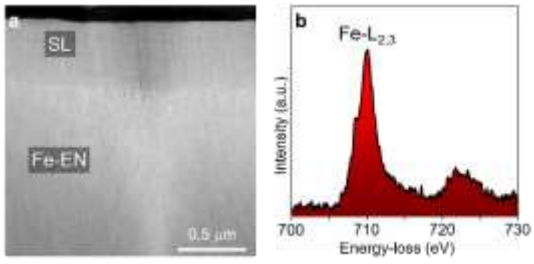

Fig. 2: (a) HAADF-STEM image of the interface between the SL and Fe-EN; (b) Fe-$L_{2,3}$ ELNES acquired from the SL.

References:
[1] P.-Y. Chen et al., Prog. Mater. Sci. **57**, 1492-1704 (2012).
[2] A. Nanci, Mosby Elsevier: St. Louis, MO, 411p. (2008).
[3] V. Srot et al., ACS Nano **18**, 11270-11283 (2024).

Prospecting for Lunar Volatiles with Abberation-Corrected STEM-EELS-EDXS

Rhonda Stroud[1*]

[1]Arizona State University, School of Earth and Space Exploration, 781 Terrace Rd, 85278, Tempe, AZ, USA

[*]rhonda.stroud@asu.edu

The surfaces of airless bodies, such as the Moon and asteroids, are exposed to charged particle irradiation and micrometeorite bombardment over time periods of hundreds to millions of years. The combined effects of the irradiation and hypervelocity particle impacts are called space weathering [1]. Space weathering features include radiation damage rims from implanted solar wind H^+ and He^+ in the top ~ 100 nm of the exposed mineral and glass regolith material, and melt deposit layers from the vaporization and redeposition of impacting grains. Observations of these effects in lunar and asteroid samples are important for constraining the evolution of rocky bodies and interpreting optical spectra from planets, and also for assessing the potential abundance of volatiles that could be extracted for technological use. Coordinated electron energy loss spectroscopy and energy dispersive x-ray spectroscopy in aberration-corrected scanning transmission electron enable direct imaging of the space weathering effects at the atomic scale and spectroscopic detection of the implanted H and He. Recent measurements show that the He concentrates in vesicles in nanophase Fe particles in silicate glasses [2], and in chromite ($FeCr_2O_4$) and ilmenite ($FeTiO_3$) [3].

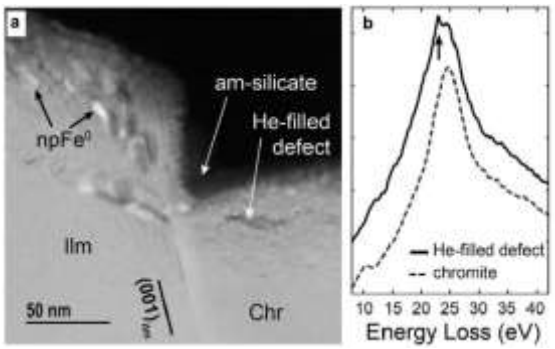

Fig. 1: a. HAADF image of a space weathered lunar soil grain with an amorphous silicate melt deposit with nano-phase metallic Fe ($npFe^0$) on adjacent ilmenite (Ilm) and chromite (Chr) grains. D. EELS measurements at the He K edge (22 eV) show solar wind He is present in the ilmenite and chromite defects. Adapted from [3].

References:

[1] C.M. Pieters, S K. J. Noble, Geophys. Res. Planet. **121**, 1865–1884 (2016).
[2] B. A. Cymes, K. D. Burgess, R. M. Stroud, Commun. Earth Environ. **5**, 189 (2024).
[3] K. D. Burgess, R. M. Stroud, Geochimica et Cosmochimica Acta **224**, 64–79, (2018).

Atomistic Insight into the Structural Differences of the η- and γ-Al_2O_3 and the Related Catalytically Active Sites

Elena Willinger[1]*, Jordan Meyet[2], Marc Georg Willinger[3], Christoph Müller[4] and Christophe Coperet[2]

[1]Technical University of Munich, Physics department, Chair of Surfacce and interface physics, Lichternberstrasse 4, 85748 Garching (Germany)
[2]ETH Zürich, Department of Chemistry and Applied Biosciences, Vladimir-Prelog-Weg 1-5/10,8093 Zürich (Switzerland)
[3]Technical University of Munich, Department of Chemistry, Chair of Electron Microscopy, Lichternberstrasse 4, 85748 Garching (Germany)
[4]ETH Zürich, Department of Maschinenbau und Verf.technik, Leonhardstrasse 21, 8092 Zürich (Switzerland)

*elena.willinger@tum.de

Transition aluminas, particularly η- and γ-Al_2O_3, are widely used in catalysis due to their high surface area and tunable acidity. Although both phases are commonly described as defective spinels, their exact crystal structures and the origins of their distinct surface properties remain debated. The transformation pathways from oxyhydroxide precursors, bayerite for η-Al_2O_3 and boehmite for γ-Al_2O_3, strongly influence their microstructure and, consequently, their surface atomistic arrangements, which ultimately govern their surface acidity.

Here, we provide direct atomistic insights into the structural differences between η- and γ-Al_2O_3 using atomic-resolution ADF-STEM imaging. We reveal that γ-Al_2O_3 can be viewed as an assembly of η-phase domains interconnected by antiphase domain boundaries (APBs) along the (100) planes. Atomic-resolution imaging shows that these APBs consist of alternating O–Al6–O and O–Al6–O–Al4 atomic rows (Fig.1).

Atomic-resolution ADF-STEM imaging further reveals that the (100) surface of γ-Al_2O_3 structurally resembles its APBs but incorporates pentacoordinated aluminum (Al5) instead of octahedrally coordinated Al6 (Fig. 2). Moreover, we found that γ-Al_2O_3 predominantly exposes (111) and (100) facets, whereas η-Al_2O_3 is mainly terminated by (111) facets and nanosteps. This distinct surface termination explains the different acidity of the two phases: γ-Al_2O_3 exhibits predominantly Lewis acidity due to undercoordinated Al sites on its (100) surfaces, while η-Al_2O_3, being exclusively (111)-terminated, presents oxygen-rich surfaces associated with dominant Brønsted acidity.

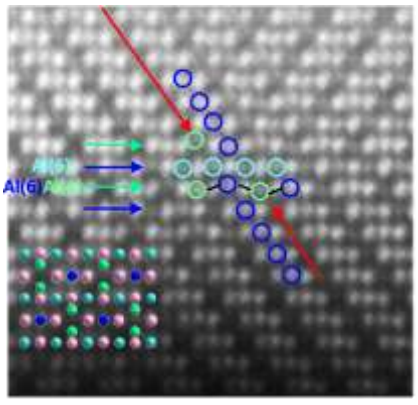

Fig. 1: ADF-STEM image of APBs of γ-Al_2O_3.

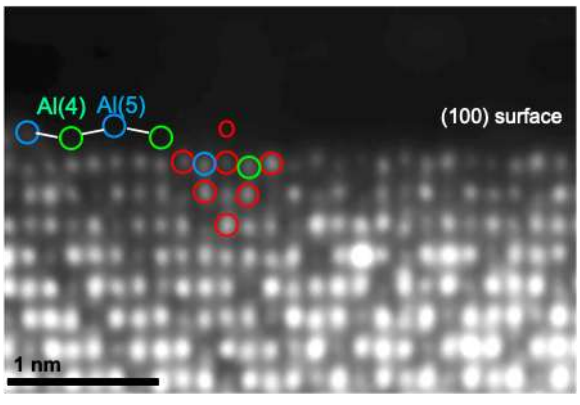

Fig. 2: ADF-STEM image of the (100)-γ-Al_2O_3 surface showing undercoordinated Al sites.

Fabrication and investigation of magnetic ring phase plates

Ulrich Poppe[1,2*], Maximilian Kruth[1], Lea Risters[1], Amir Hossein Tavabi[1], Rafal Dunin-Borkowski[1]

[1]Forschungszentrum Juelich, Ernst Ruska-Centre for Microscopy and Spectroscopy with Electrons, Juelich, Germany
[2] CEOS GmbH, Heidelberg, Germany

[*]u.poppe@fz-juelich.de

In order to enhance phase-contrast especially for biological specimens in cryo-TEM phase plates of many different designs can be used to provide a 90° phase shift between scattered and unscattered electrons [1]. Apart from a variety of phase plates which relay on a different electrical potential for the direct e-beam and scattered electrons, magnetic ring phase plates using the Aharonov-Bohm effect have been investigated mainly by Edgcombe and co-workers with thin film rings of cobalt [2]. Magnetized micro rings usually can be transferred into a state of lowest energy with azimuthal flux where the magnetic flux is confined within the magnetic material in the form of a closed loop (vortex state) and a vanishing B-field outside of the ring. The phase shift is proportional to the magnetic flux through the cross section of the magnetic material and independent from the energy of the electrons.
As often used quite insulating SiN membranes usually generate problems with charging, we used a SiC freestanding tripod supporting structure for amorphous soft magnetic $Fe_{67}Si_{18}Co_{14}B_1$ thin film rings deposited on it. As commercial SiC membranes from Norcada show a relatively low electrical conductivity (ca. 1 Ω.cm sheet resistance, high thermal conductivity and thermally stable up to 800 C°) the charging should be much less severe.
We started from SiC membrane chips with a thickness of 1 µm which were covered by a 30-50 nm thick highly permeable $Fe_{67}Si_{18}Co_{14}B_1$ thin film and protected by a ca.10 nm Pt layer. This thin film covered SiC membranes were modified by cutting structured holes with FIB to produce micro rings hold by tripod arms in a ca. 50 µm aperture hole for the scattered electrons (see Fig.1a). The micro ring had holes with a diameter between 0.5 and 1.5 µm for the direct e-beam and outer ring diameters between 2-3 µm. The soft magnetic film was removed in the FIB by ion etching between 60 and 100 nm deep on a diameter of ca.70 nm except a central region with micro rings in the centre (see example in the detail Fig.1b).
On the sample holder a VCSEL micro laser diode shining on the SiC membrane is mounted in order to change the magnetization by temperature of the magnetic ring and therefore producing an adjustable phase shift. Heating also can prevent charging by contamination.
First results of holographic investigations on described thin film rings with a few rad phase shifts and a macroscopic magnetic tube producing very large phase shifts will be presented.

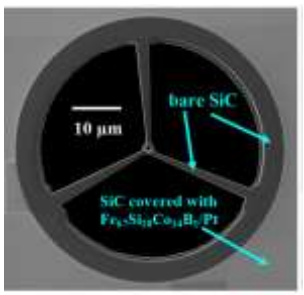

Fig. 1a: SEM picture of phase plate

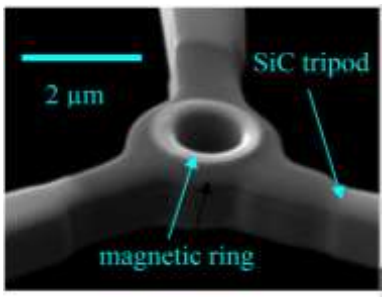

Fig. 1b: Detail with magnetic ring

References:
[1] M. Malac et al., Microscopy, **70**, 75–115, (2021)
[2] C. Edgcombe et al., Ultramicroscopy **120,** p.78 (2012).

Quantitative comparison of resolution limits: critical specimen thickness in cryo-TEM, EFTEM, and iDPC-STEM

Ciqi Liao[1*], Daniel Mann[1], Iris von der Hocht[1], Max Leo Leidl[2], Knut Müller-Caspary[2] and Carsten Sachse[1,3]

[1]Forschungszentrum Jülich, Ernst Ruska Center 3, Wilhelm Johnen Straße 52428 Jülich, Germany
[2]Ludwig Maximilians Universität München, Department of Chemistry, Butenandstr. 11, 81377 Munich, Germany
[3]Heinrich Heine Universität Düsseldorf, Mathematisch-Naturwissenschaftliche Fakultät, Universitätsstraße 1, 40225 Düsseldorf Germany

[*]c.liao@fz-juelich.de

Cryogenic electron microscopy (cryo-EM) is capable of visualizing beam sensitive biological samples at atomic resolution. However, excessive ice thickness introduces significant challenges: elastic scattering signals decay exponentially with increased sample thickness, leading to diminished image contrast, elevated noise levels, and ultimately reduced resolution and interpretability of 3D reconstruction. Specifically, energy losses from inelastic scattering events induce chromatic blurring in conventional post-specimen transmission electron microscopy (TEM), thus degrading image coherence. Energy filter transmission electron microscopy (EFTEM) can partially solve these chromatic artifacts but also decreases resolution. Notably, scanning transmission electron microscopy (STEM) offers a distinct geometric advantage in correcting chromatic aberrations. Recently, the integrated differential phase contrast (iDPC)-STEM has been shown to reach near atomic resolution in biological ice-embedded samples. iDPC-STEM is designed to be linear for thin, weakly scattering specimens and yields a signal that directly interpretable as projected electrostatic potential. Consequently, iDPC-STEM may be more suitable to larger thickness than typical cryo-TEM permits, as it can tune convergence semi-angle resulting in a change depth of focus, and use depth-sectioning to preserve contrast from the depth ranges of interest.

Therefore, we aim to systematically evaluate the impact of specimen thickness on the attainable resolution of tobacco mosaic virus (TMV) in three distinct electron microscopy modalities: TEM, EFTEM and STEM. By quantifying resolution thresholds across these imaging modes, this work seeks to identify the critical thickness at which chromatic aberration and inelastic scattering effects exert the most pronounced limitation on contrast and final resolution.

References:
[1] Lazić, I.; Wirix, M.; Leidl, M. L.; de Haas, F.; Mann, D.; Beckers, M.; Pechnikova, E. V.; Müller-Caspary, K.; Egoavil, R.; Bosch, E. G. T.; Sachse, C. Single-Particle Cryo-EM Structures from iDPC–STEM at near-Atomic Resolution. Nat. Methods 2022, 19 (9), 1126–1136. https://doi.org/10.1038/s41592-022-01586-0.
[2] Li, X.; Lazić, I.; Huang, X.; Wirix, M.; Wang, L.; Deng, Y.; Niu, T.; Wu, D.; Yu, L.; Sun, F. Imaging Biological Samples by Integrated Differential Phase Contrast (iDPC) STEM Technique. J. Struct. Biol. 2022, 214 (1), 107837. https://doi.org/10.1016/j.jsb.2022.107837.

Quantifying carbon site switching dynamics in GaN by electron holography

Keyan Ji[1], Michael Schnedler[1*], Qianqian Lan[1], Rafal E. Dunin-Borkowski[1], Philipp Ebert[1]

[1]Ernst Ruska Centrum (ER-C-1), Forschungszentrum Jülich GmbH, 52425 Jülich, Germany

[*]m.schnedler@fz-juelich.de

Carbon is ubiquitously present during metal–organic vapor phase epitaxy (MOVPE) of group-III nitride semiconductors and throughout subsequent device processing, yet its impact on electronic properties and long-term device stability remains insufficiently understood. While carbon has been implicated in degradation mechanisms (e.g., in laser diodes), it is also deliberately introduced to form semi-insulating layers for suppressing leakage and increasing breakdown voltage in high-electron-mobility transistors. However, the underlying dynamic point-defect processes and reactions involving carbon are still poorly quantified, limiting both degradation understanding and durability optimization.

We probe carbon-related point defect reactions in GaN by quantifying the time- and temperature-dependent evolution of near-surface Fermi-level pinning during annealing using electron holography in a transmission electron microscope. As model system, thin lamellas were prepared by focused ion beam (FIB) milling from a silicon-doped *n*-n^+ GaN junction grown by MOVPE on *c*-plane freestanding GaN with low dislocation density. FIB preparation leads to near-surface carbon implantation and TRIM simulations indicate an exponentially decaying carbon profile extending ~15 nm into the lamella with concentrations exceeding the doping level.

Carbon preferentially substitutes nitrogen (C_N) which in GaN exhibits a (- / 0) charge transition level at ~0.7 eV above the valence band. In *n*-type GaN this induces Fermi-level pinning and pronounced upward band bending near the surface, dominating the phase contrast captured by EH. Upon low-temperature annealing, the pinning is lifted. From the kinetics of the annealing-induced change, we identify the atomic process responsible for depinning as a short-range event with a jump length on the order of one lattice constant, accompanied by charge reversal consistent with a site-switching of carbon from substitutional to interstitial configuration. The extracted activation barrier is (2.27 ± 0.26) eV. [1]

These results establish electron holography as a quantitative approach to identify and parameterize point-defect reactions in GaN. The revealed kinetics of carbon-related site switching provide a basis for understanding carbon-driven electronic instability and offer a pathway to assess and mitigate degradation processes in nitride-based devices.

References:

[1] K. Ji, *et al.*, Phys. Rev. Research **7**, 013200 (2025)